Application of Clustering Method in Different Geophysical Parameters for Researching Subsurface Environment

Dr. Cuong Van Anh LE[1,2], Dr. Ngan Nhat Kim NGUYEN[1,2], Thuan Van NGUYEN[1,2]

[1)] University of Science, Ho Chi Minh City, Vietnam; email: lvacuong@hcmus.edu.vn
[2)] Vietnam National University Ho Chi Minh City, Ho Chi Minh City, Vietnam

http://doi.org/10.29227/IM-2022-02-05

Submission date: 13-08-2022 | Review date: 19-11-2022

Abstract

Safety of construction needs knowledge of physical parameters as stiffness or porosity of the subsurface environment. Combination of different geophysical methods such as electrical resistivity imaging and multichannel analysis of surface waves can provide distributions of resistivity and shear velocity which are responsible for the underground physical parameters. Their joint interpretation can solve individual problems of none-uniqueness of the solutions when expressing two inversion results to describe environment characteristics. In our work, the k-means clustering method can categorize the two parameters into specific zones that can help to interpret the geophysical data effectively. Our workflow consists of two stages in which two independent geophysical data are inverted and the k-means clustering is applied to the two results for achieving the specified groups. The collocated geophysical data are measured in District 9, Ho Chi Minh City, Vietnam. Matching with the geology drillhole information, the joint results generally present layered medium with the upper zone having smaller resistivity and shear velocity values and the bottom zone of stronger stiffness.

Keywords: *Electrical Resistivity Imaging, MASW, K-means Clustering*

Introduction

Colocation of different geophysical data is important in remedying non-uniqueness of solutions issue and improving accuracy of their interpretation (Le et al., 2019, Gallardo and Meju, 2004, Le et al., 2016a, Haber and Oldenburg, 1997, Moorkamp, 2017). Like minerals, hydrocarbon, ground water and hydrothermal sectors, civil construction have also applied multichannel analysis of surface wave (MASW) and electrical resistivity imaging (ERI) survey methods for validating stiffness of shallow underground environment (Mahajan et al., 2015).

ERI method can investigate electrical resistivity characteristics of a medium for tracking variation of stiffness of soil rock, existence of groundwater or distribution of geological formations (Telford et al., 1990, Sharma, 1995, Hamzah et al., 2007, Costall et al., 2018, Sikandar et al., 2010, Loke and Barker, 1995). Besides, MASW method can produce shear wave velocity model that can evaluate stability of soil rocks in civil engineering. The low velocity can respond to weak areas whereas the high one can guarantee the harder environment.

For interpreting the environment structures, geophysical joint/cooperative inversion is used for constraining each inverted geophysical (Gallardo and Meju, 2004, Gallardo and Meju, 2011, Le et al., 2016a, Le et al., 2019). Cross-gradient constraints or prior model constraints (Gallardo and Meju, 2004, Gallardo and Meju, 2011, Le et al., 2016a, Le et al., 2019) can utilize their individual geometry for solving problems of none-uniqueness of the solutions.

For enhancing data interpretation, our research purpose is to link two geophysical parameters through using defining each lithology setting after having independent inverted model. The two geophysical methods are electrical resistivity imaging and multichannel analysis of surface wave (Sauvin et al., 2011, Wisén and Christiansen, 2005, Cardarelli et al., 2014). The method for joining two geophysical models as resistivity and velocity is k-means clustering in which each lithological type can be represented of one or two k-means clusters (Le et al., 2016a, Le et al., 2019).

In our research, distribution of resistivity and shear velocity in a high-tech park, Ho Chi Minh City, Vietnam, is built for evaluating soil foundation structures. K-means clustering applied to the models can illustrate layers of clay and sands with different level of stiffness in terms of their inverted geophysical values.

Study area

Being the east gate of Ho Chi Minh City (HCMC), Thu Duc City plays a role as the newly emerging socioeconomic factor connecting Ho Chi Minh City with other southeast Provinces. Our geophysical survey including seismic and resistivity data was conducted in the One Hub project (Fig. 1), a high-tech park for examination of its soil foundation structures.

The subsurface geological materials of HCMC are divided into two main lithological units as Pleistocene and Holocene sediments (Le et al., 2020, Nguyen, 2016, Nguyen et al., 2022). The shallow geology information of the One Hub project area can consist of five layers: (i) the soil cover, (ii) dark gray silty clay, being plastic flow with depth from 1.5 to 5 meter, (iii) yellow or brown mixture of clay and sand being soft plastic, (iv) clay or sandy clay with gray-white, yellow brown, red-brown being plastic hard in the depth over 5 meter to over 20 meter, and (v) yellow sand, sand mixed with gravel (Nguyen et al., 2022).

The survey length for collocated measurement of the electrical resistivity imaging and MASW methods is 170 m. Three drill holes was setup for understanding lithology structures up to 30 m.

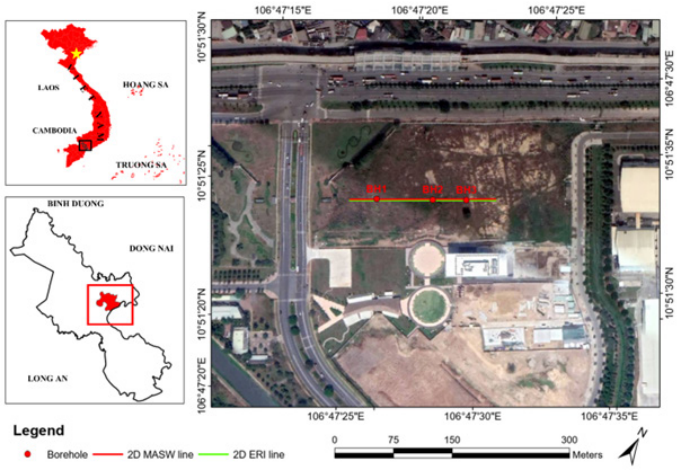

Fig. 1. Survey map and Vietnam map

Rys. 1. Mapa geodezyjna i mapa Wietnamu

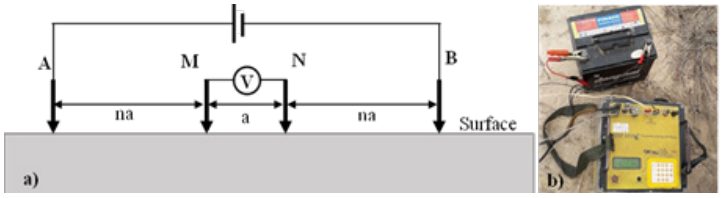

Fig. 2. a. Wenner-Schlumberger array with geometric factor K = πn(n+1)a; b. MiniSting R1 meter (AGI, 2022)

Rys. 2. a. Tablica Wennera-Schlumbergera z czynnikiem geometrycznym K = πn(n+1)a; b. Miernik MiniSting R1 (AGI, 2022)

Methodology

Our workflow focuses on three parts: (i) building electrically conductivity model from geoelectric method, (ii) setting up shear velocity model from the multichannel analysis of surface wave method, and (iii) clustering the two models for limited meaningful groups reflecting underground soils.

Electrical resistivity imaging: building electrically conductivity model

We would mainly use the geo-resistivity method to investigate the electrically conductivity of underground structures. The technique needs to collect the potential differences between two points on the ground with two or more additional electrodes after injecting an electric current into the ground through two electrodes (Loke and Barker, 1995, Loke, 1999). Ratio between the potential differences and the electric current is a measurement of the electrical resistance of the soil material known as apparent resistivity, (Loke and Barker, 1995, Loke, 1999) (Fig. 2). The 2D survey length is 170 m. Then, the data analysis process as inversion is applied to build the electrically resistivity model for delivering the answer to the project about soil stability and stiffness of the interest area.

The principle of the ERT is to solve the famous relation as known as Ohm law in calculating electrically conductivity distribution (Mufti, 1976, Akca, 2016, Telford et al., 1990, Ghanati et al., 2020):

$$\vec{J} = \sigma \vec{E} \tag{1}$$

The electric field and potential difference between two points on the ground can be related through the equation:

$$\vec{E} = -\nabla \Phi \tag{2}$$

Moreover, gradient of current density versus three axes (i.e., x, y, and z) has relationship with current as the equation below:

$$\nabla . J = \left(\frac{I}{\Delta V}\right) \delta(x - x_s)\delta(y - y_s)\delta(z - z_s) \tag{3}$$

where J electrically current density, σ electrically conductivity, E electric field, ΔV the volume. The Dirac delta function, δ(a), is shown as

$$\delta(a) = \begin{cases} 1 \; if \; a = 0 \\ 0 \; if \; a \neq 0 \end{cases}$$

Combination of the three equations (1), (2), and (3) can lead to the general equation (4):

$$-\nabla \bullet [\sigma(x,y,z))\nabla \Phi(x,y,z)] = \left(\frac{I}{\Delta V}\right) \delta(x - x_s)\delta(y - y_s)\delta(z - z_s) \tag{4}$$

Equation (4) which express the calculation of potential difference are dependent on conductivity model if the prior current is known play a crucial role as modeling stage in inversion procedure (Mufti, 1976, Akca, 2016).

Inversion is minimization of the objective function for building resistivity model after reducing difference between the real data and synthetic data (see Fig 3) (Meju, 1994).

In our research work, the source code Elris (Akca, 2016) is used for inverting the geoelectric data. Smooth constrain is used in minimizing the object function presented in the forming update model:

$$\Delta m_i = (J^T W_d^T W_d J + \lambda C)^{-1} (J^T W_d^T W_d \Delta d - \lambda C m_{i-1}) \tag{5}$$

Where Δm_i the model update showing variation of old and new values in a position, J the Jacobian matrix, λ the damping

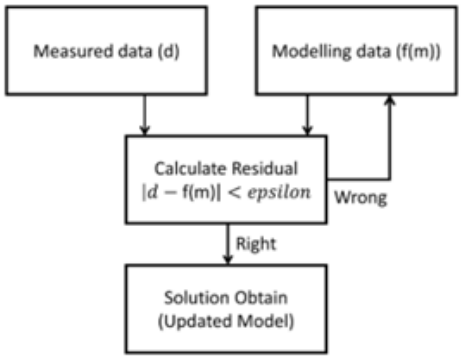

Fig. 3. Inversion procedure (Meju, 1994)
Rys. 3. Procedura inwersji (Meju, 1994)

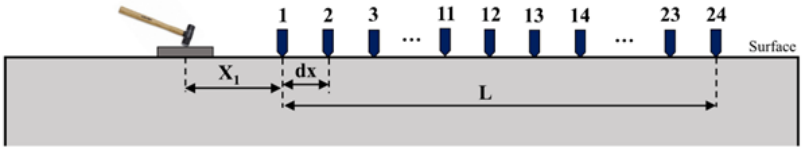

Fig. 4. MASW survey map with representation of active source (i.e., hammer) and 24 geophones
Rys. 4. Mapa pomiarowa MASW z przedstawieniem aktywnego źródła (tj. młota) i 24 geofonów

factor, Δd data discrepancy, i expressing the iteration number, W_d data weighting matrix relating to the standard deviation of data recordings, C the five-point finite difference Laplace (Mufti, 1976, Akca, 2016).

MASW theory

Raleigh waves as surface seismic wave are often seen as noises in conventional seismic methods as refraction or reflection. However, the surface waves are very useful in investigations of soil stiffness (Xia et al., 1999, Park et al., 2018). They are created from interaction of P and S waves at ground surface. The Raleigh equation (6) expresses their contributions as follows (Novotny, 1999):

$$\left(2-\frac{c^2}{V_S^2}\right)^2 = 4\left(1-\frac{c^2}{V_P^2}\right)^{\frac{1}{2}}\left(1-\frac{c^2}{V_S^2}\right)^{\frac{1}{2}} \quad (6)$$

where, c is Raleigh seismic wave velocity, Vs and Vp are shear and primary velocities, respectively.

The modelling function F (Xia et al., 1999, Schwab and Knopoff, 1972) is responsible for building the Raleigh waves dispersion curves in a layered earth model:

$$F(f, c, V_S, V_P, \rho, h) = 0 \quad (7)$$

where, c is known as the Raleigh velocity, f as frequency, V_S as shear velocity, V_P as compressional P wave velocity, ρ as density, and h as thickness.

In our paper, the active MASW mode was utilized by placing the multiple receivers (i.e., Seistronix RAS-24 geophones (Seistronix)) along a 2D survey line with single shots. For each shot, a seismograph is formed from vibrations measured by 24 geophones. Geophone spacing, sampling rate and record length were set at 1 m, 0.25 ms and 1 s, respectively (Fig. 4). The source offsets were sequentially set at 5 m to the left of the first geophone (Fig.4). A 9-kg sledgehammer was employed to knock on the metal plate to generate the seismic waves.

Inversion procedure: Dispersion curves are extracted from seismogram datasets measurement in the field. The curves expressing relation between phase Raleigh velocity versus frequency are input for the inversion procedure. Inversion approach is to build the shear velocity model in terms of reducing misfit of the synthetic and real data of phase Raleigh velocity. Minimization of the object function (equation 7) and shear wave velocity model can be conducted (Xia et al., 1999):

$$\Phi = \|J\Delta x - \Delta b\|W\|J\Delta x - \Delta b\| + \alpha\|\Delta x\|^2 \quad (8)$$

$$\Delta x = V(\Lambda^2 + \alpha I)^{-1}\Lambda U^T d \quad (9)$$

Where, x represents solution of shear wave velocity, b shows measured phase Raleigh velocity, J as Jacobian matrix expressing the first derivative function of Raleigh velocity versus shear velocity, and α is damping factor. Δb is the difference between the synthetic and real data of phase Raleigh velocity. W is the covariance matrix relating measured error and $W=L^T$ L. Δx is the difference of the initial model and updated model. Matrixes V and Λ are calculated from A=LJ and decomposition of $A=U\Lambda V^T$. d=Lb. I is the unit matrix.

For updating the shear velocity model from the measured MASW data, we have used the PS software (Park Seismic LLC, 2022) to investigate shallow underground structures. The MASW inversion procedure follows the scheme discussed in Fig. 3.

K-means approach

K-means, an effective clustering approach, is well-tested and easily executed in many geophysical research areas (Di Giuseppe et al., 2014, Le et al., 2016b, Zhao et al., 2015, Shen et al., 2005). In Lindsten et al. (2011)'s work, the idea for K-means clustering technique was first proposed by Hugo Steinhaus in 1957. Its main idea "minimises the sum, over all clusters, of the within-cluster sums of point-to-cluster-centroid distances" (MathWorks, 2014) and its equations are presented below (Lindsten et al., 2011, Le, 2017):

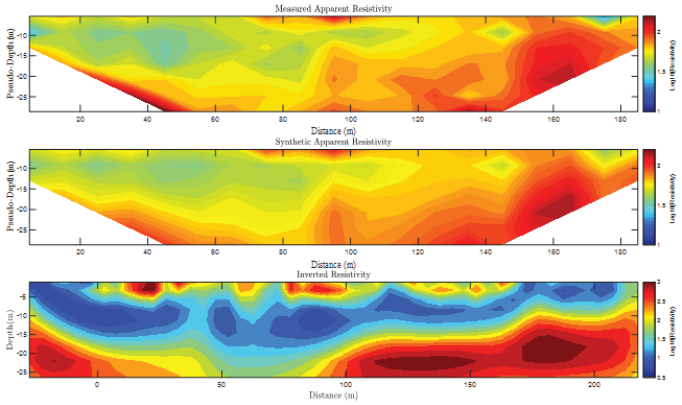

Fig. 5. Distribution of Resistivity for the survey area. The top image represents the measured apparent resistivity, the middle image shows the synthetic data and the below image is the inverted resistivity model after using Elris source (Akca, 2016)

Rys. 5. Rozkład rezystywności dla badanego obszaru. Górny obraz przedstawia zmierzoną rezystywność pozorną, środkowy obraz pokazuje dane syntetyczne, a poniższy obraz to odwrócony model rezystywności po użyciu źródła Elris (Akca, 2016)

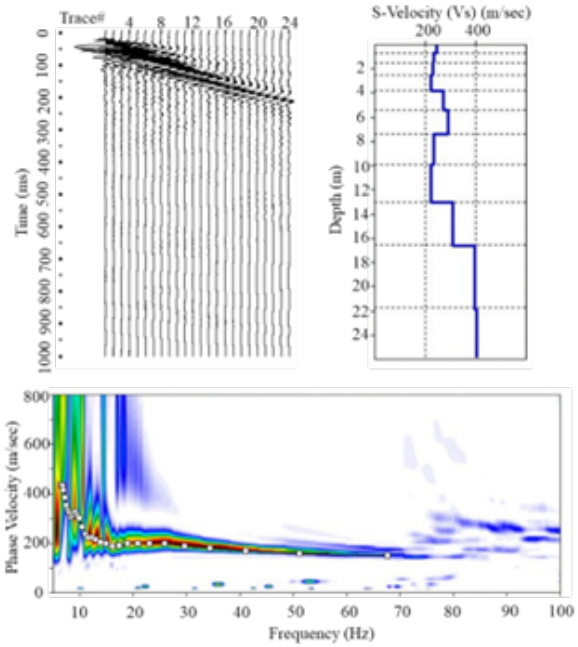

Fig. 6. Seismic data, dispersion curve (Raleigh phase velocity), and 1D VS profile extracted from the MASW inversion of BH1

Rys. 6. Dane sejsmiczne, krzywa dyspersji (prędkość fazowa Raleigha) i profil 1D VS wyodrębniony z inwersji MASW BH1

$$E = \sum_{i=1}^{k} \sum_{i=1}^{n_i} d(x_{ij}, m_i) \quad (10)$$

$$d(x_{ij}, m_i) = (x_{ij} - m_i)(x_{ij} - m_i)^T \quad (11)$$

where E, an objective function (Shen et al., 2005), is the sum of square-errors for all data observations, x_{ij} the jth observation in the ith cluster, m_i the center value or mean of the cluster I, n_i the total number of observations in each cluster i, and k the number of clusters (Lindsten et al., 2011).

Four steps in the k-means approach are listed below:

Step 1: K cluster centroids is initially chosen

Step 2: Allocate new observations belong to one cluster with the closest centroid.

Step 3: Updating the new values of the centroids from Step 2 or new centroid for each cluster is computed.

Step 4: Repeating the step 2 until the new centroids are not changed.

The way to choose the optimal cluster of k-means algorithm can follows some mathematical criterion (Davies and Bouldin, 1979) or lithology information extracted from drill holes (Le et al., 2016a, Le et al., 2019).

Results and discussion

We have collected the geophysical data as MASW data and geoelectric data. Their collocated profile length is 170 meters. Noise filters for each data are applied prior running inversion. The inverted results are input for clustering procedure.

ERI result

The 2D ERI data was collected by the MiniSting R1 meter manufactured by Advanced Geosciences Inc (AGI, 2022) and using a Wenner-Schlumberger configuration (Fig.2.) (Nguyen et al., 2022). The first sequence of spacing factor (n) is 1 with a minimum of electrode spacing is 10 m. The last sequence of a spacing factor equals 7 corresponding to the median depth of investigation about 28.5 m (Edwards, 1977).

The Elris code (Akca, 2016) follows the smoothness inversion style for producing the resistivity model. The starting mod-

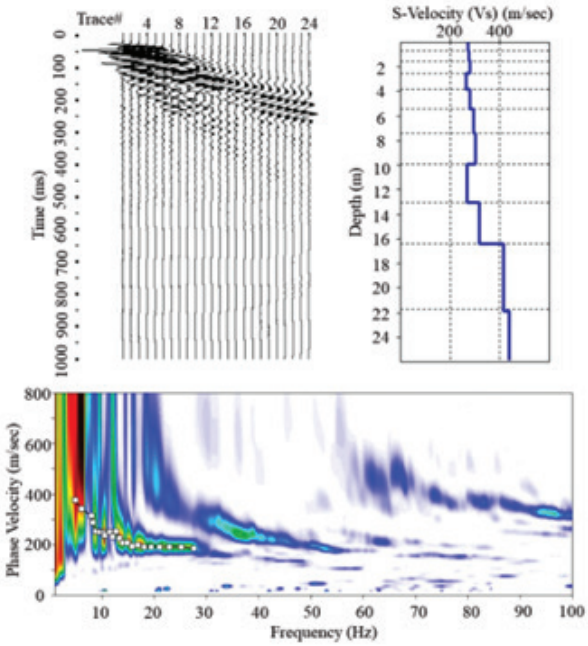

Fig. 7. Seismic data, dispersion curve (Raleigh phase velocity), and 1D VS profile extracted from the MASW inversion of BH2
Rys. 7. Dane sejsmiczne, krzywa dyspersji (prędkość fazowa Raleigha) i profil 1D VS wyodrębniony z inwersji MASW BH2

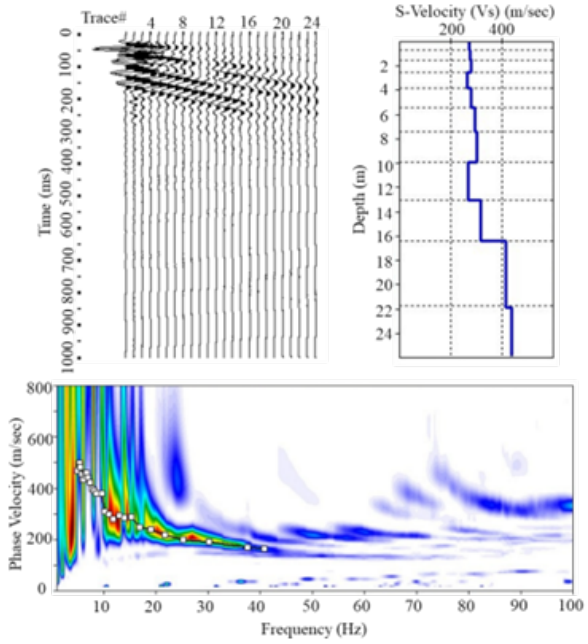

Fig. 8. Seismic data, dispersion curve (Raleigh phase velocity), and 1D VS profile extracted from the MASW inversion of BH3
Rys. 8. Dane sejsmiczne, krzywa dyspersji (prędkość fazowa Raleigha) i profil 1D VS wyodrębniony z inwersji MASW BH3

el is the homogenous model with the constant value extracted from the background resistivity as 66 Ω.m. After 19 iterations, data difference between real and synthetic data is 14.53%.

The resistivity model presents three distinct layers with the maximum depth as 25 m. The first layer can be interpreted as the cover with about 100 Ω.m, the second layer is responsible for the most conductive one, and the third layer is the most resistive (Fig. 5).

MASW result

The analysis of the MASW-method data is conducted as three steps (See Figs. 6, 7, and 8):

The seismic records were loaded into the PS software (Park Seismic LLC, 2022) to display and transform the raw data to phase velocity-frequency spectrum to get the dispersion images. In this study, the frequency and phase velocity were set in the range of 0 -100 Hz and 1-800 m/s, respectively.

Manual process for picking the peaks values from the dispersion image is to generate the dispersion curve. This dispersion curve is the real data for MASW inversion approach in building shear velocity model.

The shear wave velocity (Vs) distribution was calculated from an iterative inversion process (Xia et al., 1999). In inversion scheme, the nonlinear least square technique is needed

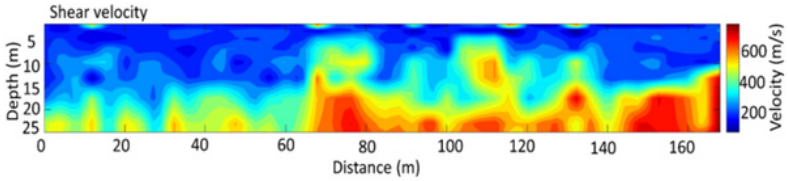

Fig. 9. MASW velocity model
Rys. 9. Model prędkości MASW

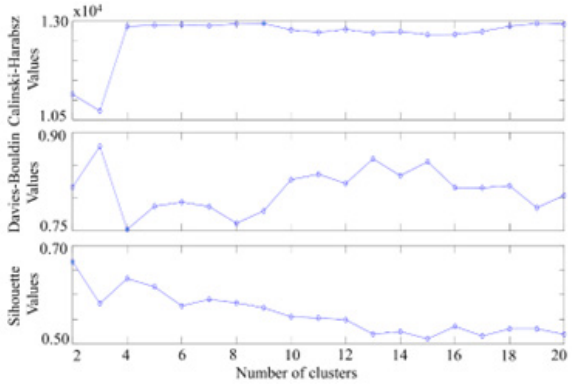

Fig. 10. Three criteria for choosing the optima numbers
Rys. 10. Trzy kryteria wyboru liczb optymalnych

to generate the 1D VS (shear wave velocity) profile in which misfit between real and synthetic data is reduced.

The 1D MASW inversion stops after 3 iterations. The match of the synthetic and real data is larger than 90%. The 1D model VS profile is divided into 11 layers from surface to the depth of 26 m (Figs. 6,7,8). Their thickness values increases versus depth (from 1 m to 6 m). The shear wave velocity ranges from 200–500 m/s.

The 2D shear velocity model (see Fig. 9) is formed from 43 1D-shear velocity curve extracted from the MASW inversion. It looks like the underground structures consists of two distinct zones as low and high shear velocity values. The low velocity zone starting from surface to 15 m depth can be divided into two sub layers while the high velocity zone is believed to correlate with zone of the high stiffness.

Clustering of ERI and MASW result

Our purpose of using k-means clustering algorithms is to figure out compatibility between our inverted geophysical results (i.e., resistivity and velocity models) with lithology information extracted from the three drill holes (BH1, BH2, and BH3).

For testing k-means clustering with these two datasets as resistivity and velocity, we have run all 19 choices with number of k-means cluster groups ranging from 2 to 20. Then, we also use three criteria for choosing the optima numbers (Fig. 10). The criteria Calinski-Harabsz, Davies-Bouldin (Davies and Bouldin, 1979), and Sihouette (Matlab, 2019) prefer the number of clusters as 9, 4, and 2, respectively.

For further interpretation about geology structures, we have plotted the input of k-means algorithm and its clustering results in Fig. 11. We also added one result processed from the cluster 7. The cluster 7 is got from number of geology sediments in three drill holes BH1, BH2, and BH3. The results from indexes 7 and 9 looks similar with structures of the geophysical data (resistivity and velocity models).

The great compatibility between lithology and 7-clustered image can prove that the validity of velocity and resistivity models (Fig. 12). Boundaries of different sediment layers are greatly matched with ones of lithology structures.

In Fig. 13, cross-plot between of two geophysical models as resistivity and velocity presents roughly three trends. One is a line parallel to the y axis (log10 of Resistivity), the other reflects the middle value of tangent angle and the one is smallest angle. It looks like there is existence of the most conductive layer with velocity varying from medium to maximum (Fig. 11).

Conclusion

Combination of the two geophysical models can enhance knowledge of the soil rock foundation which is useful for safety of construction. The interest environment are k-means analyzed with different clustering indexes. The seven clusters are chosen for processing. In the results, there only six lithology within the specified depth 25 m. Interestingly, one important conductive but average to largest velocity values exist and below 20 m, one layer of being highly resistive and maximum velocity is the most stiffness. The collocated geophysical data are measured in District 9, Ho Chi Minh City, Vietnam. The results reflect high stability of the soil where layers of clay and sands with strong stiffness are homogenous.

Acknowledgments: This research is funded by University of Science, VNUHCM under grant number T2022-52. We are also grateful to dGB Earth Sciences and Curtin University for providing access to software tools.
Conflicts of Interest: The authors declare no conflict of interest.
Author Contribution: All authors contribute to data processing and writing the manuscript. CVAL mainly write the manuscript. NNKN processed MASW data, NVT and CVAL processed ERI data. CVAL processed clustering and lithology interpretation.

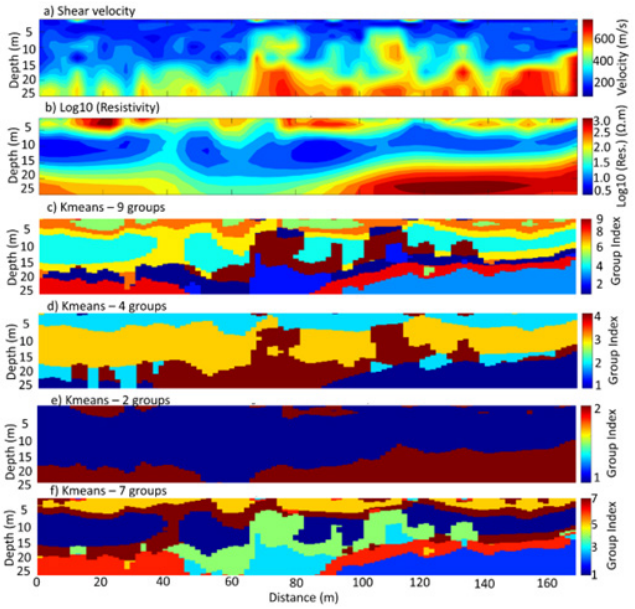

Fig. 11. Resistivity and Velocity and clustering results of different k-means

Rys. 11. Wyniki rezystywności i prędkości oraz grupowania różnych k-średnich

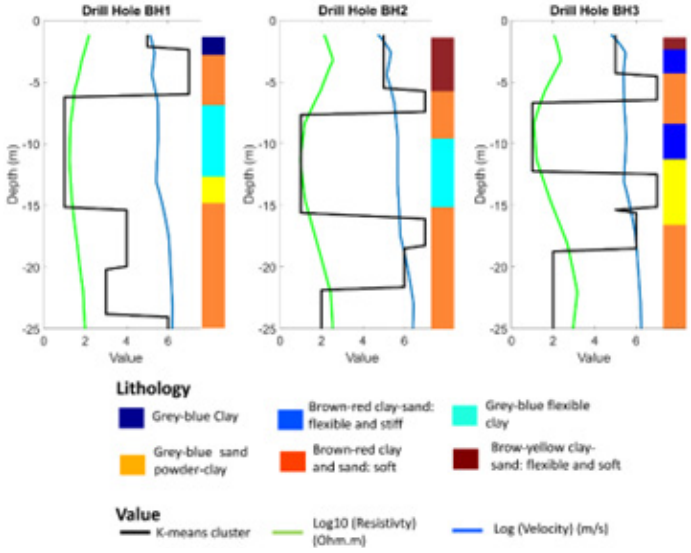

Fig. 12. Representation of Resistivity and Velocity, clustering results versus depth in the three drill holes, BH1, BH2, and BH3

Rys. 11. Wyniki rezystywności i prędkości oraz grupowania różnych k-średnich

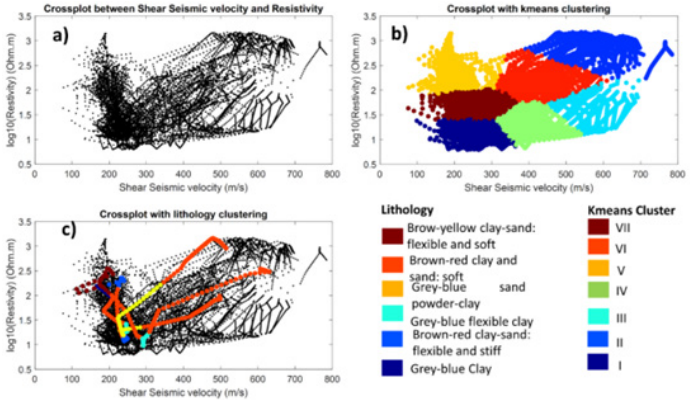

Fig. 13. Cross-plot of Resistivity and Velocity with and without overlaid information of k-means clusters which is extracted from 7-index and lithology information

Ryc. 13. Wykres krzyżowy rezystywności i prędkości z i bez nałożonych informacji o klastrach k-średnich, który jest wyodrębniony z 7-indeksów i informacji litologicznych

Literatura – References

1. AGI. 2022. MiniSting [Online]. Available: https://www.agiusa.com/ministing 2022].
2. AKCA, I. 2016. ELRIS2D: A MATLAB Package for the 2D Inversion of DC Resistivity/IP Data. Acta Geophysica, 64, 443-462.
3. CARDARELLI, E., CERCATO, M. & DE DONNO, G. 2014. Characterization of an earth-filled dam through the combined use of electrical resistivity tomography, P-and SH-wave seismic tomography and surface wave data. Journal of Applied Geophysics, 106, 87-95.
4. COSTALL, A., HARRIS, B. & PIGOIS, J. 2018. Electrical resistivity imaging and the saline water interface in high-quality coastal aquifers. Surveys in geophysics, 39, 753-816.
5. DAVIES, D. L. & BOULDIN, D. W. 1979. A Cluster Separation Measure. IEEE Transactions on Pattern Analysis and Machine Intelligence.
6. DI GIUSEPPE, M. G., TROIANO, A., TROISE, C. & DE NATALE, G. 2014. k-Means clustering as tool for multivariate geophysical data analysis. An application to shallow fault zone imaging. Journal of Applied Geophysics, 101, 108-115.
7. EDWARDS, L. 1977. A modified pseudosection for resistivity and IP. Geophysics, 42, 1020-1036.
8. GALLARDO, L. A. & MEJU, M. A. 2004. Joint two-dimensional DC resistivity and seismic travel time inversion with cross-gradients constraints. Journal of Geophysical Research: Solid Earth, 109.
9. GALLARDO, L. A. & MEJU, M. A. 2011. STRUCTURE-COUPLED MULTIPHYSICS IMAGING IN GEOPHYSICAL SCIENCES. Reviews of Geophysics.
10. GHANATI, R., AZADI, Y. & FAKHIMI, R. 2020. RESIP2DMODE: A MATLAB-Based 2D Resistivity and Induced Polarization Forward Modeling Software. Iranian Journal of Geophysics, 60-78.
11. HABER, E. & OLDENBURG, D. 1997. Joint inversion: a structural approach. Inverse problems, 13, 63.
12. HAMZAH, U., SAMSUDIN, A. R. & MALIM, E. P. 2007. Groundwater investigation in Kuala Selangor using vertical electrical sounding (VES) surveys. Environmental geology, 51, 1349-1359.
13. LE, C. V. A. 2017. Cooperative Inversion of Magnetotelluric and Seismic Data. Doctor of Philosophy, Curtin University.
14. LE, C. V. A., DUONG, M. B. & KIEU, T. D. 2020. High–Resolution Seismic Reflection Survey of Holocene Sediment Distribution at Thi Vai River, Ho Chi Minh City, Vietnam. Lecture Notes in Civil Engineering. Springer.
15. LE, C. V. A., HARRIS, B. D. & PETHICK, A. M. 2019. New perspectives on Solid Earth Geology from Seismic Texture to Cooperative Inversion. Scientific Reports, 9, 14737.
16. LE, C. V. A., HARRIS, B. D., PETHICK, A. M., TAKAM TAKOUGANG, E. M. & HOWE, B. 2016a. Semiautomatic and Automatic Cooperative Inversion of Seismic and Magnetotelluric Data. Surveys in Geophysics, 37, 845-896.
17. LE, C. V. A., HARRIS, B. D., PETHICK, A. M., TAKOUGANG, E. M. T. & HOWE, B. 2016b. Semiautomatic and Automatic Cooperative Inversion of Seismic and Magnetotelluric Data. Surveys in Geophysics, 37, 845-896.
18. LINDSTEN, F., OHLSSON, H. & LJUNG, L. 2011. Just relax and come clustering!: A convexification of k-means clustering.
19. LOKE, M. & BARKER, R. 1995. Least-squares deconvolution of apparent resistivity pseudosections. Geophysics, 60, 1682-1690.
20. LOKE, M. H. 1999. Electrical imaging surveys for environmental and engineering studies. A practical guide to 2-D and 3-D surveys.
21. MAHAJAN, A., CHANDRA, S., SARMA, V. & ARORA, B. 2015. Multichannel analysis of surface waves and high-resolution electrical resistivity tomography in detection of subsurface features in northwest Himalaya. Current Science, 2230-2239.
22. MATHWORKS. 2014. MATLAB [Online]. Available: http://au.mathworks.com/help/stats/k-means-clustering.html 2014].
23. MATLAB. 2019. silhouette [Online]. Available: https://www.mathworks.com/help/stats/silhouette.html 2022].
24. MEJU, M. A. 1994. Geophysical data analysis: Understanding inverse problem theory and practice, Society of Exploration Geophysicists.
25. MOORKAMP, M. 2017. Integrating Electromagnetic Data with Other Geophysical Observations for Enhanced Imaging of the Earth: A Tutorial and Review. Surveys in Geophysics, 1-28.
26. MUFTI, I. R. 1976. Finite-difference resistivity modeling for arbitraily shaped two-dimensional structures. Geophyscs, 41, 62-78.

27. NGUYEN, N. K. N., NGUYEN, V. T., VO, M. K., DINH, Q. T. & NGUYEN, Q. D. 2022. Application of electrical imaging and multichannel analysis of surface waves methods to survey the structure foundation at the Districts 2 and 9 of Ho Chi Minh City. Science and Technology Development Journal-Natural Sciences, 6, 1801-1810.
28. NGUYEN, Q. T. 2016. The main causes of land subsidence in Ho Chi Minh City. Procedia engineering, 142, 334-341.
29. NOVOTNY, O. 1999. Seismic surface waves. In: INSTITUTO DE FISICA, I. D. G. (ed.). Bahia, Salvador.
30. PARK, B., KIM, J., LEE, J., KANG, M.-S. & AN, Y.-K. 2018. Underground object classification for urban roads using instantaneous phase analysis of ground-penetrating radar (GPR) data. Remote Sensing, 10, 1417.
31. PARK SEISMIC LLC. 2022. ParkSeis (c) (PS) [Online]. Available: https://www.parkseismic.com/psoverview/ 2022].
32. SAUVIN, G., BAZIN, S., VANNESTE, M., LECOMTE, I. & PFAFFHUBER, A. Towards joint inversion/interpretation for landslide-prone areas in Norway-integrating geophysics and geotechnique. Near Surface 2011-17th EAGE European Meeting of Environmental and Engineering Geophysics, 2011. European Association of Geoscientists & Engineers, cp-253-00052.
33. SCHWAB, F. & KNOPOFF, L. 1972. Fast surface wave and free mode computations. Methods in computational physics: advances in research and applications. Elsevier.
34. SEISTRONIX. RAS-24 Exploration Seismograph [Online]. Available: http://www.seistronix.com/ras_g.htm 2022].
35. SHARMA, P. 1995. Environmental and Engineering Geophysics.
36. SHEN, J., CHANG, S. I., LEE, E. S., DENG, Y. & BROWN, S. J. 2005. Determination of cluster number in clustering microarray data. Applied Mathematics and Computation, 169, 1172-1185.
37. SIKANDAR, P., BAKHSH, A., ARSHAD, M. & RANA, T. 2010. The use of vertical electrical sounding resistivity method for the location of low salinity groundwater for irrigation in Chaj and Rachna Doabs. Environmental Earth Sciences, 60, 1113-1129.
38. TELFORD, W. M., TELFORD, W., GELDART, L. & SHERIFF, R. E. 1990. Applied geophysics, Cambridge university press.
39. WISÉN, R. & CHRISTIANSEN, A. V. 2005. Laterally and mutually constrained inversion of surface wave seismic data and resistivity data. Journal of Environmental and Engineering Geophysics, 10, 251-262.
40. XIA, J., MILLER, R. D. & PARK, C. B. 1999. Estimation of near-surface shear-wave velocity by inversion of Rayleigh waves. Geophysics, 64, 691-700.
41. ZHAO, T., JAYARAM, V., ROY, A. & MARFURT, K. J. 2015. A comparison of classification techniques for seismic facies recognition. Interpretation.

Zastosowanie metody klastrowania w różnych parametrach geofizycznych do badania środowiska podpowierzchniowego

Bezpieczeństwo konstrukcji wymaga znajomości parametrów fizycznych, takich jak sztywność czy porowatość środowiska podpowierzchniowego. Połączenie różnych metod geofizycznych, takich jak obrazowanie rezystywności elektrycznej i wielokanałowa analiza fal powierzchniowych, może dostarczyć rozkłady rezystywności i prędkości ścinania, które są odpowiedzialne za parametry fizyczne podziemnych warstw. Ich wspólna interpretacja może rozwiązać indywidualne problemy niejednoznaczności rozwiązań przy wyrażaniu dwóch wyników inwersji do opisu cech środowiska. W naszej pracy metoda grupowania k-średnich może podzielić dwa parametry na określone strefy, co może pomóc w skutecznej interpretacji danych geofizycznych. Nasz przepływ pracy składa się z dwóch etapów, w których dwa niezależne dane geofizyczne są odwracane, a grupowanie k-średnich jest stosowane do dwóch wyników w celu uzyskania określonych grup. Zebrane dane geofizyczne są mierzone w Dystrykcie 9, Ho Chi Minh City, Wietnam. Dopasowując się do informacji uzyskanych z odwiertów geologicznych, wyniki połączeń ogólnie przedstawiają ośrodek warstwowy, w którym górna strefa ma mniejsze wartości rezystywności i prędkości ścinania, a dolna strefa ma większą sztywność.

Słowa kluczowe: *obrazowanie oporności elektrycznej, MASW, grupowanie K-średnich*